Computers & Structures Vol. 16, No. 1–4, pp. 167–185, 1983
Printed in Great Britain

0045-7949/83/010167-19$03.00/0
Pergamon Press Ltd.

PANDA—INTERACTIVE PROGRAM FOR MINIMUM WEIGHT DESIGN OF STIFFENED CYLINDRICAL PANELS AND SHELLS

DAVID BUSHNELL†
Lockheed Palo Alto Research Laboratory, 3251 Hanover Street, Palo Alto, CA 94304, U.S.A.

Abstract—An analysis and an interactive computer program are described through which minimum weight designs of composite, elastic-plastic, stiffened, cylindrical panels can be obtained subject to general and local buckling constraints and stress and strain constraints. The panels are subjected to arbitrary combinations of in-plane axial, circumferential and shear resultants. Nonlinear material effects are included if the material is isotropic or has stiffness in only one direction (as does a discrete or a smeared stiffener).

Several types of general and local buckling modes are included as constraints in the optimization process, including general instability, panel instability with either stringers or rings smeared out, local skin buckling, local crippling of stiffener segments, and general, panel and local skin buckling including the effects of stiffener rolling. Certain stiffener rolling modes in which the panel skin does not deform but the cross section of the stiffener does deform are also accounted for.

The interactive PANDA system consists of three independently executed modules that share the same data base. In the first module an initial design concept with rough (not necessarily feasible or accurate) dimensions are provided by the user in a "conversational" mode. In the second module the user decides which of the design parameters of the concept are to be treated by PANDA as decision variables in the optimization phase. In the third module the optimization calculations are carried out. Examples are provided in which optimum designs obtained by PANDA are compared to those in the literature.

INTRODUCTION

Objective

The objective of the development of PANDA has been to create an interactive computer program for engineers which derives minimum weight designs of stiffened cylindrical panels under combined in-plane loads, N_x, N_y and N_{xy}. The loading of the stiffened panel is assumed in most cases to result in uniform membrane strain components e_x and e_y in both skin and stiffeners and uniform shear strain e_{xy} in the skin. Meridional bending between rings in the prebuckling phase is included for shells without axial stiffeners. Nonlinear material behavior is included in the prebuckling analysis if the material is isotropic or has strength only in one direction (smeared or discrete stiffeners).

Buckling loads are calculated by use of simple assumed displacement functions used in conjunction with Donnell-type kinematic relations[1]. For example, general instability of panels with balanced laminates and no shear loading is assumed to occur in the familiar $w(x, y) = C \sin(ny) \sin(mx)$ mode. In the presence of in-plane shear and/or unbalanced laminates, both local and general buckling patterns are assumed to have the form

$$w(x, y) = C\{\cos[(n + mc)y - (m + nd)x] - \cos[(n - mc)y + (m - nd)x]\} \quad (1)$$

in which either c or d are zero, depending on the geometry and the stiffness of the entire panel or whatever portion of the panel is under consideration.

The skin is cylindrical with radius R and the stiffeners are composed of assemblages of flat plate segments the axial lengths of which are large compared to the heights and the heights of which are large compared to the thicknesses. These flat plate segments are oriented either normal or parallel to the plane of the panel skin. Figure 1 shows an example of the panel geometry. The overall dimensions of the panel are (a, b) and the spacings of the stiffeners are (a_0, b_0).

Optimization is accomplished by means of the widely used CONMIN routine developed by Vanderplaats[2–4].

Brief review of the literature

This review is concerned with optimization of stiffened shells and panels under destabilizing loads. Optimization techniques *per se* are not discussed or referenced here. Venkayya[5] has written an excellent survey with an extensive bibliography on this subject.

Most of the work on optimization of stiffened shells and panels under compressive loads has been motivated by the wish to find minimum weight designs of aerospace vehicles. Minimum weight designs of ship decks and submarine pressure hulls have also been studied. In recent years computer programs for optimizing aerospace structures have been written for application to laminated wall construction. Design variables include laminae thicknesses and winding angles. Computer programs for optimizing ship structures, especially submarine pressure hulls, have been written to include nonlinear material behavior.

Optimization algorithms have tended to follow either of two strategies: (1) calculation of optimum designs from linear or nonlinear programming techniques created to find minima of an objective function in design space, and (2) calculation of optimum designs from formulas derived from the condition that different types of failures should occur at a given load. (See Venkayya[5] for further details.)

†Staff Scientist.

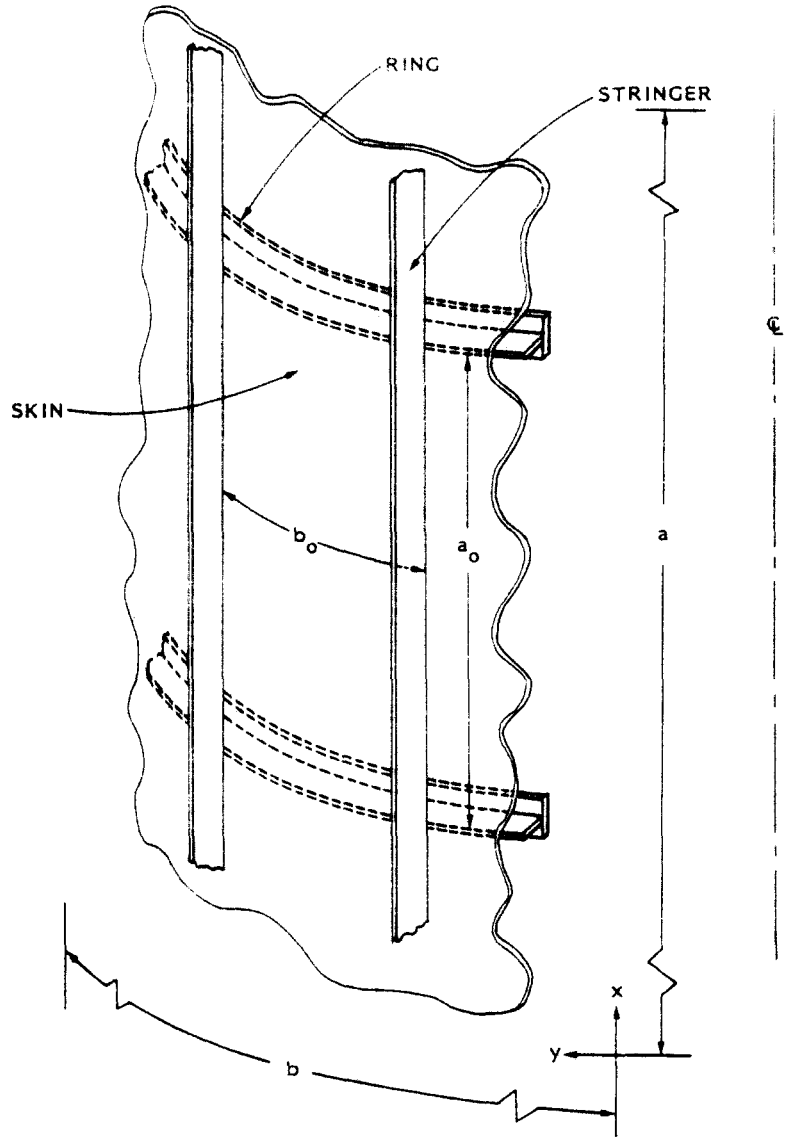

Fig. 1. Stiffened cylindrical panel with overall dimensions (a, b), ring spacing (a_0) and stringer spacing (b_0).

One of the earliest papers on optimum design of stiffened panels is by Catchpole[5a]. Schmit and his colleagues have written several papers on optimization of stiffened plates and cylindrical shells subject to combined in-plane loading[6–10]. Optimization is by various nonlinear programming methods. In an early work, Schmit *et al.*[6] found minimum weight designs of rectangular, simply supported waffle plates. Buckling constraint conditions include general instability, local instability between stiffeners and stiffener instability. Bronowicki *et al.*[10] optimized a cylindrical shell with internal T-shaped rings subject to uniform external hydrostatic pressure. They found minimum weight designs with maximum separation of the lowest two frequencies and with maximum separation of the lowest two frequencies with primarily axial content. Gross buckling is prevented by specification of a minimum natural frequency. Additional constraints preclude yielding, buckling of panels between rings and buckling of stiffeners or stiffener segments. Optimization is by use of a sequential unconstrained minimization technique.

Several papers were written by Burns and his colleagues[11–15]. The primary motivation was to produce minimum weight designs of rocket boosters. The structures were optimized through application of formulas which dictate that local and general instability occur at the same load.

Many articles and computer programs have been written under the sponsorship of NASA or used by NASA personnel[16–26]. The motivation has been to design minimum weight structures and to provide computer programs for the design of rocket boosters and airplane fuselages and wings.

The latest in the series of NASA programs for optimization of aerospace structures is the PASCO program[26, 27] written by Anderson, Stroud, and others at NASA. This program calculates minimum weight designs of composite stiffened panels. A panel is considered to be built up of an assemblage of flat plate segments, each of which may have laminated wall construction. The buckling analysis is exact within the limitations of Kirchoff-Love theory. Thus, complex

buckling modes are included in the optimization process, modes for example in which general and local waviness are combined. The panels must be simply supported at the top and bottom and be stiffened only in the axial direction. The effects of bow-type imperfections are included, both in the stress and local buckling analyses. PASCO is a combination of a structural program VIPASA written by Wittrick and Williams[23] for the local and general buckling of stiffened flat panels and the previously mentioned optimization routine CONMIN written by Vanderplaats[2].

Recent advances in the application of laminated composite materials to aerospace structures has led to many papers on the optimization of stiffened composite panels and wings, among them [28–31].

Several papers on optimization of stiffened cylinders have been written recently by Simitses and his colleagues[32–36]. Their primary motivation has been to produce a computerized capability to design minimum weight fuselages for large aircraft. These structures are subjected to combined axial compression, shear and internal pressure. In the papers by Simitses *et al.* the buckling equations are based on Donnell's shell theory[1]. The Galerkin procedure is used to obtain buckling loads. The series expansion for the buckling modal displacement is valid for simply supported panels. Local buckling of stiffener segments is included, and both rings and stringers may be present. The von Mises yield criterion is used for the maximum stress constraint. Optimization is by a variation of the Simplex method.

Dickson *et al.*[37] have written a computer program for the minimum-weight design of composite, stiffened flat panels loaded into the far-post-buckling range by any combination of in-plane biaxial compression or tension and shear. They extended a post buckling theory for isotropic plates developed by Koiter in 1946[38] for isotropic plates in their analysis of the locally post buckled panel and they performed optimization via Vanderplaats' routine CONMIN[2–4].

Papers have been written on the optimization of structures used in ships[39–47]. While recent developments in capabilities to create minimum weight designs of aerospace structures have emphasized laminated composites, recent developments of capabilities to create minimum weight designs of ships have included nonlinear material behavior[44]. Optimization programs for the minimum weight design of submarine pressure hulls (ring stiffened cylinders) have been written by Pappas and his co-workers[45–47] and by Renzi[44]. Renzi's program, called DAPS3, essentially incorporates the structural analysis and concepts described in [40–43]. Pappas[47] includes in his optimization program general instability, buckling between rings and crippling of the rings, which have T-shaped cross sections. The design is constrained by a maximum stress criterion and the material must remain elastic. Pappas performs an elaborate search in buckling modal wavelength space (m, n)-space in order to obtain reliably the minimum buckling load corresponding to general instability.

Under the sponsorship of the Air Force Flight Dynamics Laboratory, Almroth *et al.*[48] have created a system of computer programs that work together to create optimum designs of stiffened cylindrical panels. The PANDA code, based on simple buckling formulas and restricted to simply supported uniform panels, can be used to obtain an initial design. The parameters of this design are stored on a file which can be read by other programs requiring more computer time than PANDA but not restricted as to boundary conditions and uniformity of thickness, stiffener spacing, loading and buckling mode shapes.

Other papers on optimization subject to constraints other than buckling and stress include Refs. [49, 50].

SCOPE OF PANDA

Material properties

If the material is orthotropic or anisotropic, buckling is assumed to occur at stress levels for which this material remains elastic. Feasible designs are constrained by maximum stress or strain criteria. Plasticity with arbitrary strain hardening is permitted if the material is isotropic or if it has stiffness in one coordinate direction only, as does the continuum representation of each segment of a smeared stiffener. The cylindrical skin and stiffener segments can be composed of multiple layers of isotropic or orthotropic material, as depicted in Fig. 2. Each layer has a unique angle of orthotropy relative in the case of the panel skin to the direction of the generator (x-direction) and in the case of a stiffener segment to the stiffener axis. In the buckling analysis the segments of the stiffeners are assumed to be monocoque and isotropic or orthotropic, not layered anisotropic. Therefore, equivalent orthotropic properties for stiffener segments are calculated from input data for the stiffener segment laminates provided by the program user.

Types of buckling

Optimum designs with respect to weight are obtained in the presence of constraints due to local and general buckling, maximum tensile and compressive stress or strain, maximum shear strain, and lower and upper bounds on skin layer thicknesses, stiffener cross section dimensions and stiffener spacings.

Design parameters allowed to vary during the optimization phase include panel skin laminae thicknesses and winding angles, spacings of stiffeners and thicknesses and widths of the segments of ring and stringer cross sections.

The buckling formulas are derived from Donnell's[1] equations with *a posteriori* application of a reduction factor $(n_c^2 - 1)/n_c^2$ for panels in which the axial half wavelength of the buckling pattern is longer than the panel radius of curvature, R. The circumferential wave index n_c equals $n\pi R/b$ or $n\pi R/b_0$, with n being the number of half waves in the circumferential direction over the span b or b_0, respectively.

The many types of buckling included in the PANDA analysis are summarized in Table 1 and are briefly described next.

Skin buckling. For the case of balanced laminates and no in-plane shear, local buckling of the skin is assumed to have the form

$$w_{\text{skin}} = C_{\text{skin}} \sin\left(\frac{\bar{n}_{\text{skin}}\,\pi y}{b_0}\right) \sin\left(\frac{\bar{m}_{\text{skin}}\pi x}{a_0}\right) \qquad (2)$$

in which $\bar{n}_{\text{skin}}$ and $\bar{m}_{\text{skin}}$ are the numbers of half-waves between stringers with spacing b_0 and rings with spacing a_0, respectively. Equation (2) implies simple support boundary conditions at stiffener lines of attachment. With shear present and/or unbalanced laminates the skin buckling pattern has the form given in eqn (1).

General instability. General instability buckling modes of panels with balanced laminates and no shear also have

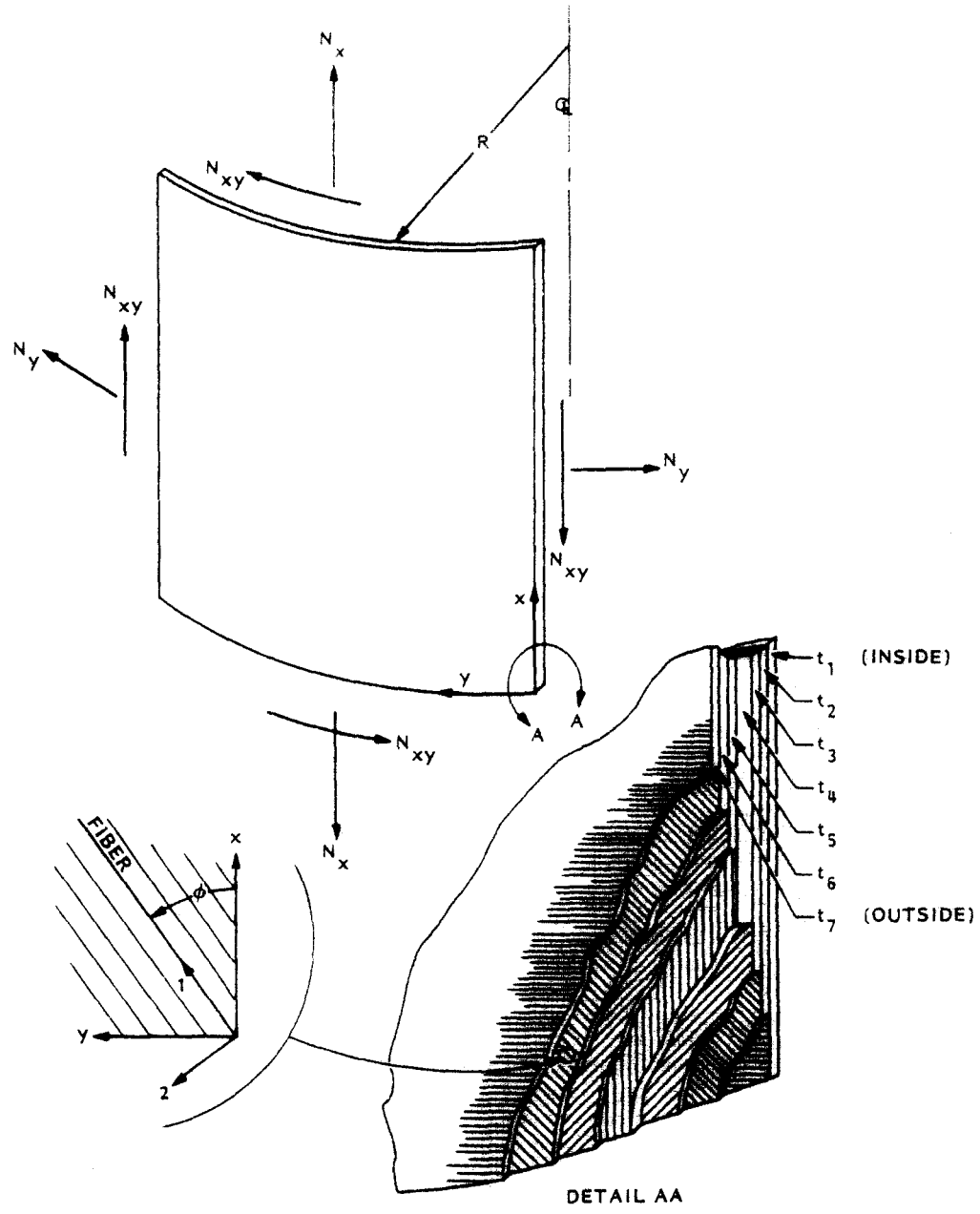

Fig. 2. Coordinates, loading and wall construction.

the form given in eqn (2) with a_0, b_0, $\bar{n}_{skin}$, $\bar{m}_{skin}$ replaced by quantities appropriate to the overall dimensions (a, b) of the panel. PANDA also calculates values for "semi-general" instability, that is buckling between rings with smeared stringers and buckling between stringers with smeared rings.

Buckling of stiffeners. Local buckling of the ith stiffener segment implies

$$w^i_{stiff} = C^i_{stiff} \sin\left(\frac{\pi \bar{y}_i}{b_i}\right) \sin\left(\frac{\bar{m}^i_{stiff}\pi\bar{x}}{l}\right) \tag{3}$$

for each stiffener segment with both long edges supported (called "internal" segments in Fig. 3). The quantity $\bar{x}$ is the coordinate along the stiffener axis; $\bar{y}_i$ is the coordinate perpendicular to $\bar{x}$ in the plane of the ith stiffener segment; b_i is the width (height) of the stiffener segment and l is the length of the stiffener segment. ($l = a_0$ for stringers and $l = b_0$ for rings). For stiffener segments with only one long edge supported, (called "end" segments), the local buckling modal displacement is assumed to be in the form

$$w^i_{stiff} = C^i_{stiff}\, \bar{y}_i \sin\left(\frac{\bar{m}^i_{stiff}\pi\bar{x}}{l}\right). \tag{4}$$

The stiffener segment buckling analysis is carried out with the assumption that each "internal" segment buck-

les with its own $\bar{m}^i$. This assumption implies that rotational incompatibility exists at junctions between segments with differing critical values of $\bar{m}^i$. "End" segments are assumed to buckle at the critical $\bar{m}^i$ of the segment to which they are joined. The buckling modes (3) and (4) are shown in Fig. 3. The coordinate $\bar{x}$ is normal to the plane of the page.

Rolling modes. Additional types of panel and stiffener buckling are considered here. These are called "rolling" modes. The first kind of rolling mode involves both skin and stiffeners and is local or "semi-general", the characteristic half-wave-length being integer fractions of the lengths (a_0, b_0), or (a, b_0) or (a_0, b). In these rolling modes the stiffener cross sections rotate about their lines of attachment to the panel skin as shown in Fig. 4(a). The cross sections do not deform in the plane of the paper. They do warp, however. The other types of rolling instability do not involve the skin at all. Only the stiffener web deforms, the rest of the stiffener cross section displacing and rotating as a rigid body, as displayed in Fig. 4(b). One of these rolling modes (Fig. 4b) occurs in both rings and stringers and in both curved and flat panels. In this mode the buckling deformations are nonuniform (sinusoidal) along the axis of the stiffener.

The other rolling mode (Fig. 4c) occurs only in the cases of internal rings on cylindrical panels under external pressure and external rings on cylindrical panels under internal pressure. In this mode buckling deformations are uniform along the axis of the ring. Stiffener rolling in the more general mode (Fig. 4b) is due to compression along the stiffener axis and is only weakly dependent on the curvature of this axis. On the other hand, the local ring buckling depicted in Fig. 4(c) is axisymmetric and arises because of the circumferential curvature of the stiffener axis and prestress in the stiffener segments. It is interesting to note that axisymmetric rolling can occur even if there are no compressive stresses anywhere in the structure.

Optimization

The subroutine CONMIN [2, 3] is used in PANDA for finding minimum weight designs. This subroutine, written

Table 1. Buckling modes included in the PANDA analysis (*contd on next page*)

TYPE OF BUCKLING	MODEL USED FOR ESTIMATE
1. General instability	Buckling of skin and stiffeners together with smeared rings and stringers. Panel is simply supported along the edges x = y = 0, x = a, and y = b.
2. Local instability	Buckling of skin between adjacent rings and adjacent stringers. Portion of panel bounded by adjacent stiffeners is simply supported. Stiffeners take their share of the load in the prebuckling analysis but are disregarded in the stability analysis.
3. Panel instability	
(a) between rings with smeared stringers	Buckling of skin and stringers between adjacent rings. Portion of panel bounded by adjacent rings is simply supported. Stringers are smeared. Simple support conditions imposed at y = 0 and at y = b. Rings take their share of the load in the prebuckling analysis, but are disregarded in the stability analysis.
(b) between stringers with smeared rings	Buckling of skin and rings between adjacent stringers. Portion of panel between adjacent stringers is simply supported. Rings are smeared. Simple support conditions imposed at x = 0 and at x = a. Stringers take their share of the load in the prebuckling analysis, but are disregarded in the stability analysis.
4. Local crippling of stiffener segments	
(a) "internal" segments	Individual stiffener segment buckles as if it were a long flat strip simply supported along its two long edges. Loading is compression along the stiffener axis. Curvature of ring segments ignored.
(b) "end" segments	Individual stiffener segment buckles as if it were a long flat strip simply supported along the long edge at which it is attached to its neighboring segment or to the panel skin and free along the opposite edge. Loading is compression along the stiffener axis. Number of half waves along the stiffener axis is the same as that of the part of the structure to which the "end" is attached. Curvature of ring segments ignored.

Table 1. (*Contd*)

TYPE OF BUCKLING	MODEL USED FOR ESTIMATE
5. Local rolling with skin buckling between stiffeners	Same as "Local instability" except that strain energy in stiffeners and work done by prebuckling compression in stiffeners are included in the buckling formula. Stiffener cross sections do not deform as stiffeners twist about their lines of attachment to the panel skin.
6. Rolling instability	
(a) with smeared stringers	Same as "Panel instability", Type (a), except that strain energy of rings and work done by prebuckling compression along the ring centroidal axis are included in the buckling formula. Ring cross section does not deform as ring twists about its line of attachment to the panel skin.
(b) with smeared rings	Same as "Panel instability", Type (b), except that strain energy of stringers and work done by prebuckling compression along the stringer centroidal axis are included in the buckling formula. Stringer cross section does not deform as it twists about its line of attachment to the panel skin.
7. Rolling of stringers, no buckling of skin	Stringer web cross section deforms but the flange cross section does not. Buckling mode has waves along stiffener axis.
8. Rolling of rings, no buckling of skin	Ring web cross section deforms but the flange cross section does not. Buckling mode has waves along the ring axis. This mode is sometimes called "frame tripping" by those interested in submarine structures.
9. Axisymmetric rolling of rings, no skin buckling	Same as "Rolling of rings", except that the buckling mode has zero waves around the circumference of the panel.

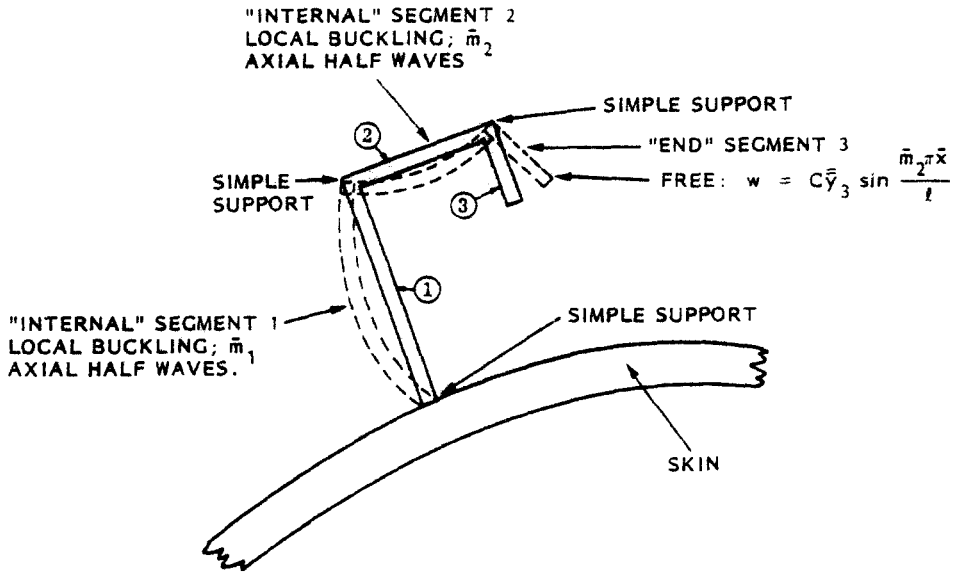

EACH "INTERNAL" STIFFENER SEGMENT IS ASSUMED TO BE SIMPLY-SUPPORTED AT ITS EDGES. THE "END" SEGMENT REMAINS STRAIGHT IN THE WIDTH COORDINATE AS SEGMENTS 2 AND 3 BUCKLE TOGETHER WITH THE SAME $\bar{m} = \bar{m}_2$.

Fig. 3. Local buckling of stiffener segments.

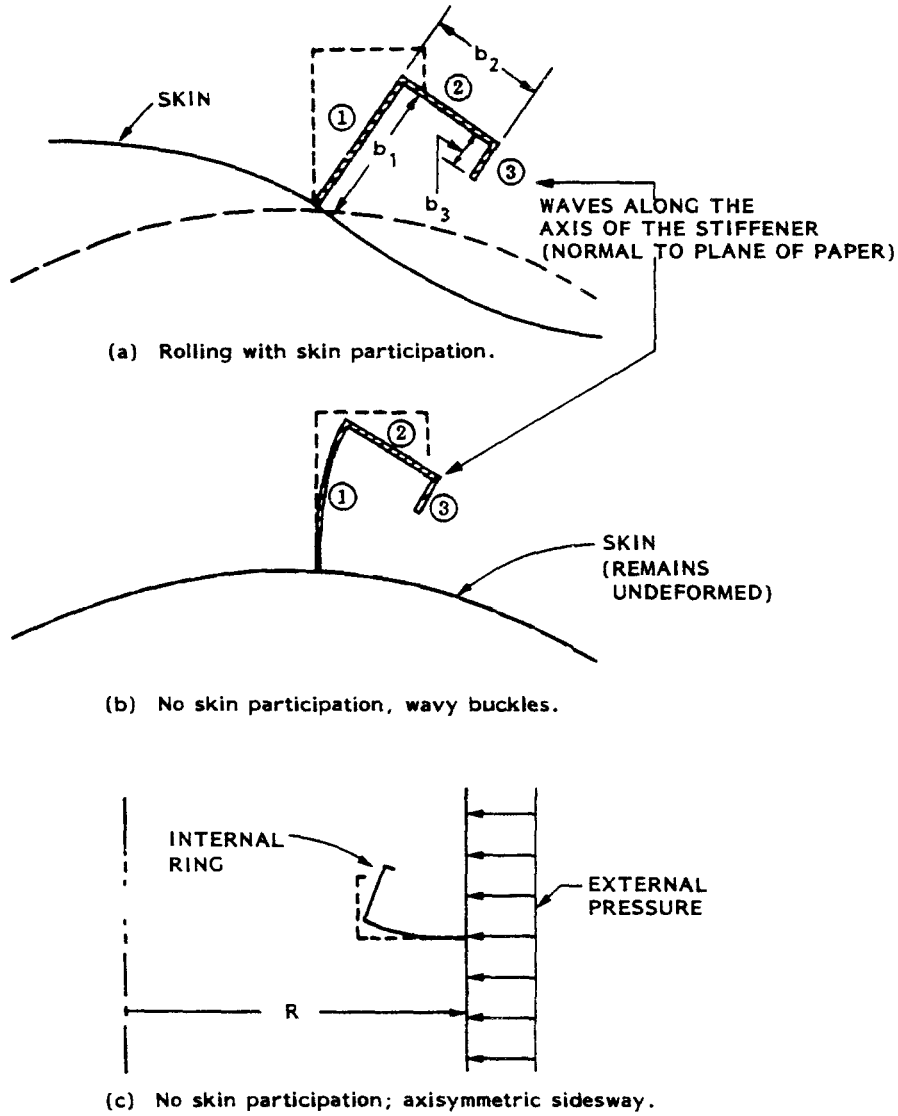

Fig. 4. Three types of "rolling" of a stiffener.

by Vanderplaats in the early 1970's, is based on a nonlinear constrained search algorithm due to Zoutendijk[4]. Briefly, the technique used in CONMIN is to minimize an objective function (panel weight, for example) until one or more constraints, in this case buckling loads, maximum stress or strain and upper and lower bounds on decision variables, become active. The minimization process then continues by following the constraint boundaries in decision variable space in a direction such that the value of the objective function continues to decrease. When a point is reached where no further decrease in the objective function is obtained, the process is terminated.

Imperfection sensitivity

It should be emphasized that PANDA does not account explicitly for initial structural imperfections. As the code is now written, the user should design a panel to higher loads than those actually to be seen in service; the deleterious effects of initial imperfections can be accounted for in this way.

Details in report

Full details of the theory on which PANDA is based are presented in [51]. Reference [51] also includes numerous examples, comparisons from the literature and the results of a parameter study on the elastic–plastic buckling of submarine hulls optimized for various pressures.

FLOW OF CALCULATIONS IN PANDA

Figures 5 and 6 show the flow of calculations in PANDA. Each of the top two boxes in Fig. 5 represents a separate interactive computer program. In the first program (called BEGIN) the user, with a specific concept in mind (e.g. knowing in advance that he wants to find the minimum weight design of a composite cylindrical shell of 7 layers stiffened by T-shaped composite internal rings and I-shaped aluminum external stringers) provides the material properties, loads and rough starting design in a "conversational" mode.

In the second program (called DECIDE) the user decides whether he wants to do simply a buckling analy-

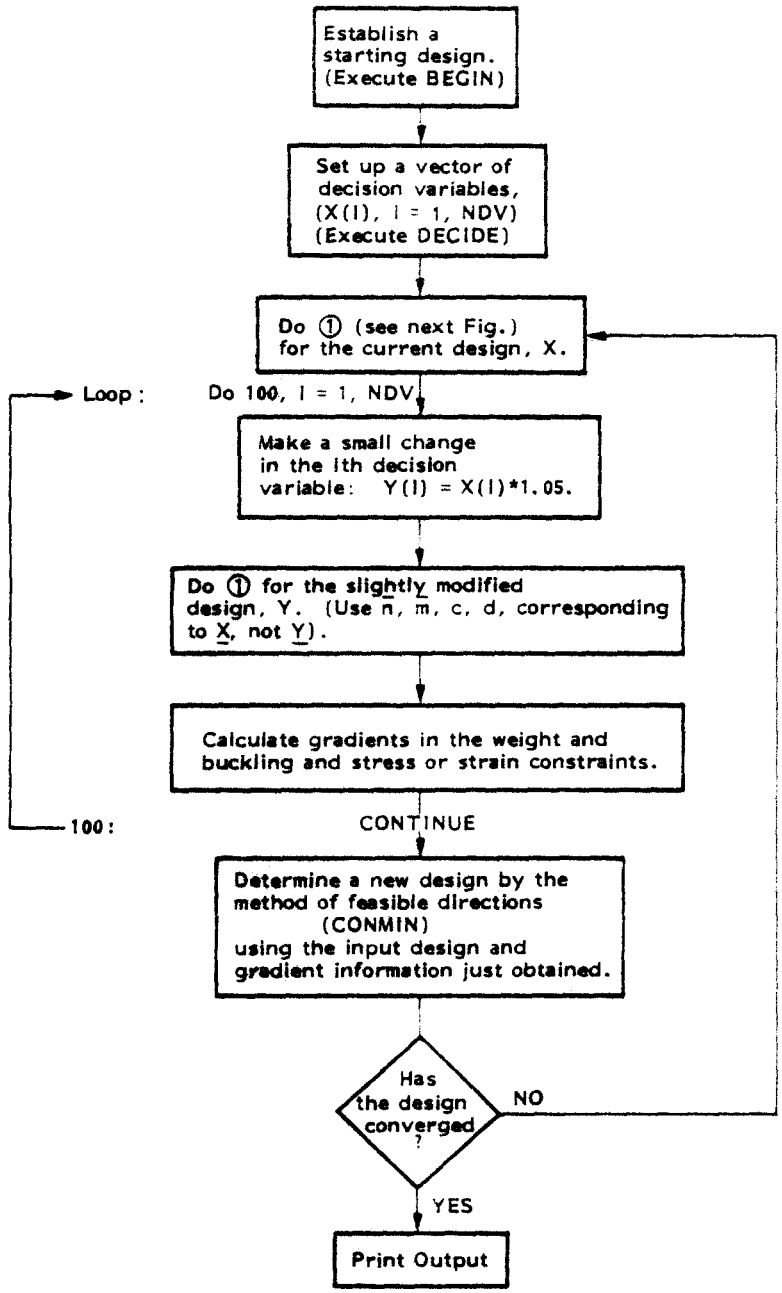

Fig. 5. Flow of calculations in PANDA for an optimization analysis.

sis of the starting design or whether he wants to do an optimization analysis. If he wants to do an optimization analysis, the user is then asked, also in this second program, to identify which of the design parameters are to be allowed to vary during the optimization process, that is, which of the design parameters are to be "decision variables" and what are the lower and upper bounds of these decision variables. The user can also specify at this time that certain of the design parameters be "linked" to (to vary in proportion with) certain of the decision variables. For example, in laminated composite wall construction the thicknesses of layers with plus winding angles are usually taken to be equal to those with minus the same winding angles.

After the first two programs have been executed the user next executes the main analysis module through the command "RUN PANCON", which performs, with some on-line interaction with the user, the rest of the calculations indicated in Figs. 5 and 6.

Prebuckling analysis

If the materials of the skin and stiffeners remain elastic at the load level specified by the designer, then the prebuckling analysis consists of:

(1) determination of the membrane strain field in the panel with smeared stiffeners;

(2) an approximate determination of the circumferential strain midway between rings and circumferential

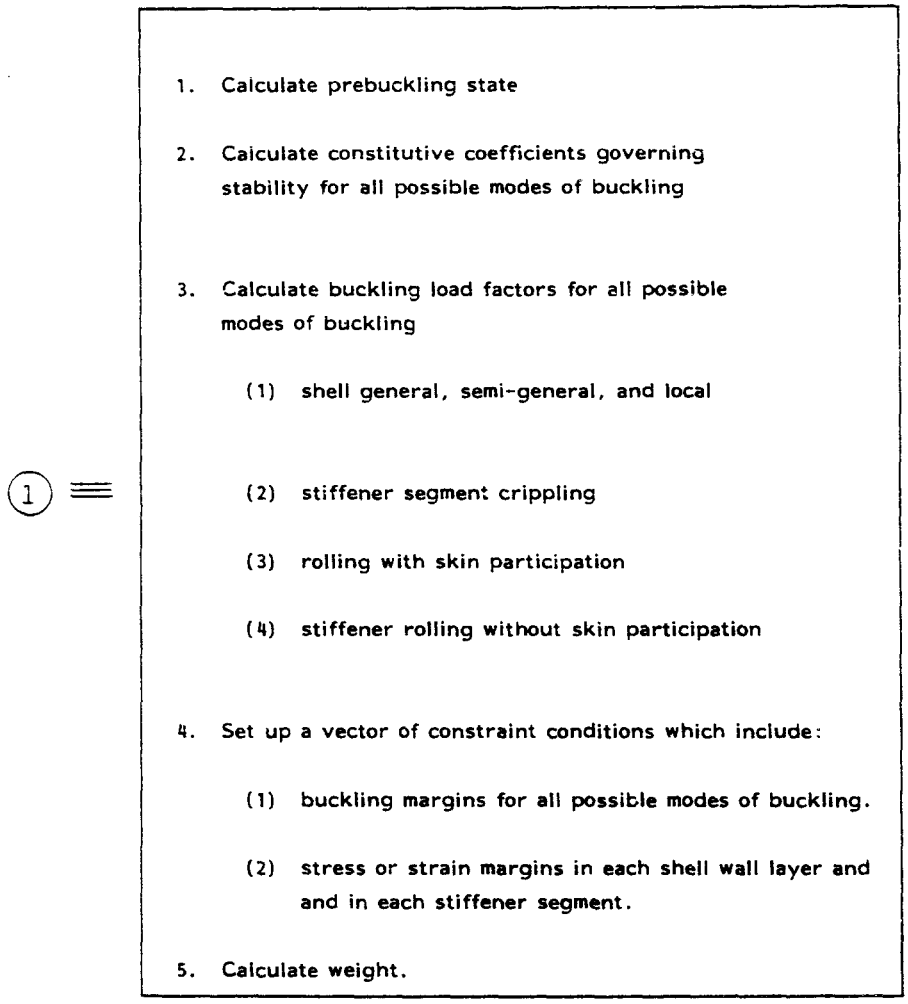

Fig. 6. The structural analysis module of PANDA. This module is embedded in the executable processor PANCON.

strain at ring centroids for panels stiffened by rings only;

(3) an approximate determination of the axial bending midway between rings; and

(4) a computation from the known strain field and known material properties of how much of the total load is carried by the skin and how much is carried by the stiffeners. (The in-plane shear load is carried only by the skin.)

In the case of panels or complete cylindrical shells stiffened by rings and subjected to uniform laterial pressure, the stress in the skin midway between rings can be rather sensitive to the ring cross section area and spacing for configurations with rather closely spaced rings. Such configurations represent optimum designs of submarine pressure hulls, for example. The buckling pressure corresponding to local instability depends directly on the midbay circumferential stress. When the material behavior is nonlinear, the buckling pressure corresponding to general instability also depends on the state of strain at midbay because the reduced moduli of the skin there naturally act to decrease the coefficients C_{ij} of the integrated constitutive law, which appear in the buckling equations.

Inclusion of plasticity. The flow of calculations in the prebuckling phase is displayed in Fig. 7. As can be seen from this flow, the process is iterative. In the presence of plastic flow, the objectives of the prebuckling computations, in addition to the four just listed for the elastic case, are:

(1) to compute instantaneous values for the reduced moduli of each layer of the panel skin, which are used to calculate the integrated constitutive law governing stability; and

(2) to compute instantaneous moduli of the segments of the rings and stringers.

These objectives are summarized in the two boxes in the lower left-hand corner of Fig. 7. Iterations at a given design state continue until the prebuckling strain components change no more than 0.01% from their values as of the previous iteration. Quadratic extrapolation of the strain components is used every four iterations.

Bifurcation buckling

It is easy to see from Fig. 5 that if there are a large number, NDV, of decision variables (NDV > 6, say) many, many buckling load factors must be computed,

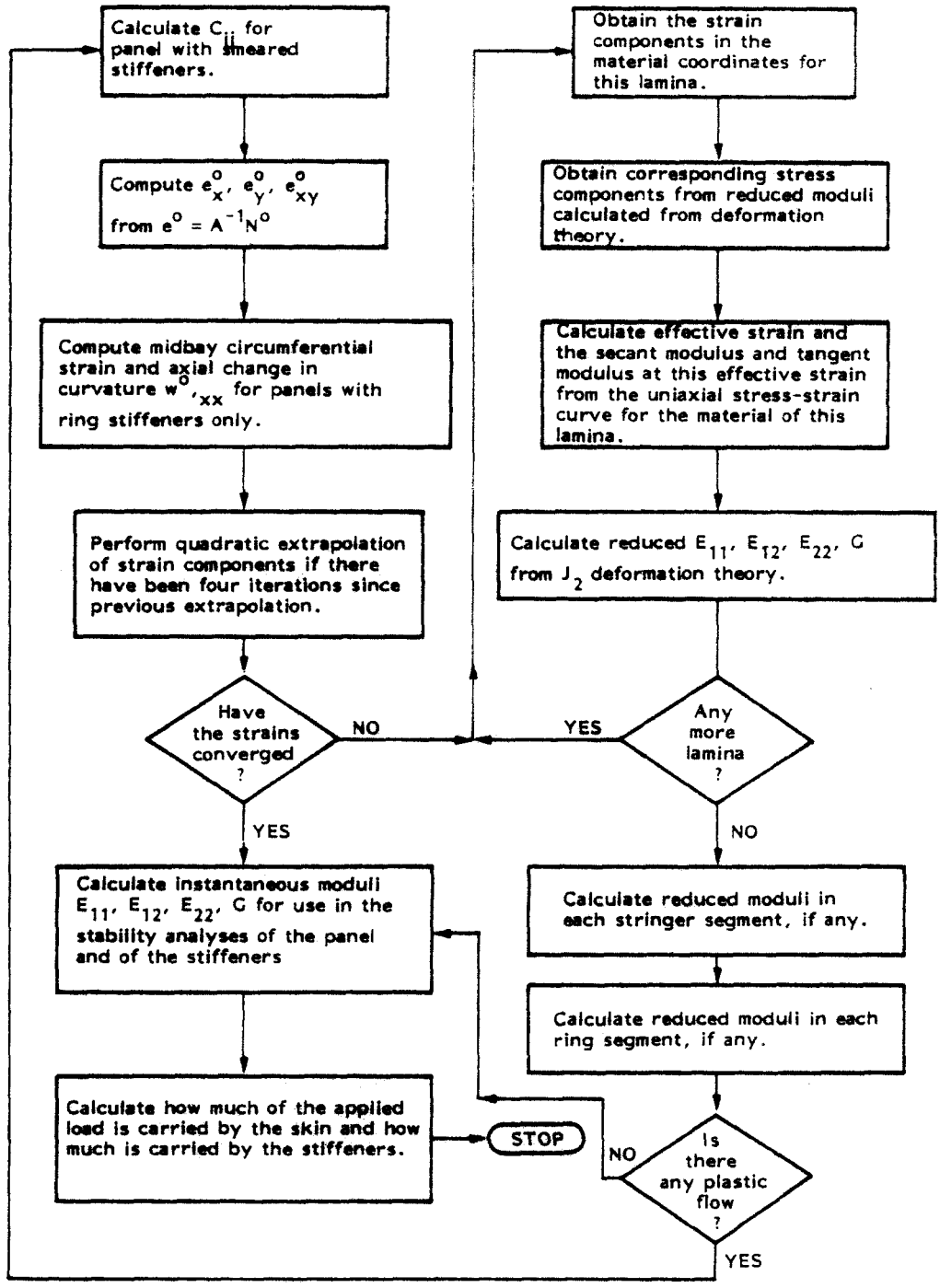

Fig. 7. Flow of calculations for Elastic-Plastic Prebuckling Analysis in PANDA.

especially if the case is complicated so that many different kinds of buckling modes must be considered. For example, in the case displayed in Fig. 8, for which 11 different types of buckling are investigated, as listed in Table 1, there might be as many as 7 decision variables: t, a_0, b_0, t^s, b^s, t^r and b^r (identified in Fig. 8). Thus, each execution of the loop, ($I = 1$, NDV), in Fig. 5 requires calculation of NDV*11 = 77 critical buckling load factors. Each of the 77 critical buckling load factors represents the results of minimization of the potential energy with respect to the wave indices m and n and the buckling nodal line slopes c or d [eqn (1)]. In order to save computer time in PANDA the buckling modal parameters, $m(i)$, $n(i)$, $c(i)$, and $d(i)$, $i = 1, 2, \ldots 11$ corresponding to the 11 critical modes for the current "baseline" design ($X(J), J = 1$, NDV) are held constant for the slightly perturbed designs Y investigated in the loop over NDV. These perturbed designs must be

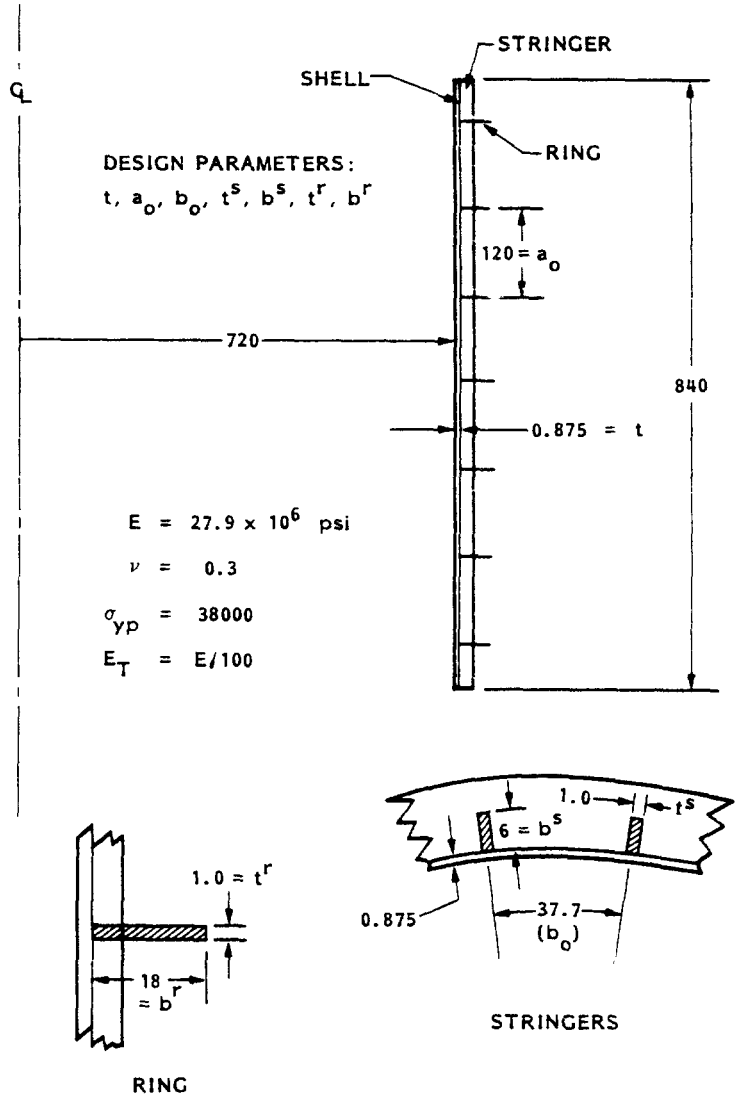

Fig. 8. Ring and stringer stiffened cylindrical shell with dimensions typical of a large containment vessel for a nuclear reactor.

evaluated with regard to stress and buckling in order to generate gradients of weight and constraint conditions needed by the optimizer CONMIN[2, 3].

VERIFICATION/EVALUATION OF PANDA

This section is divided into two subsections: (1) buckling predictions for fixed designs, and (2) results from optimization analyses. Answers from PANDA are compared with those from the literature.

Buckling predictions from PANDA for fixed designs

Purpose of this section. The purpose of this section is to provide the reader with an idea of the quality of the estimates of buckling loads for the many kinds of instability summarized in Table 1. Many more examples appear in Ref. [51].

The accuracy of PANDA buckling predictions is case dependent; expressions such as (1) cannot lead to predictions with uniform accuracy for differing configurations. The emphasis during the development of PANDA was on the creation of an interactive *preliminary* design tool that includes many kinds of buckling yet responds rapidly on a minicomputer such as the VAX. PANDA can be used very effectively to reduce greatly the vast expanse of feasible design space to a manageable region. This region can subsequently be explored further with the use of more elaborate design programs that require more computer time, such as that described in Ref. [48].

Buckling loads of isotropic unstiffened panels and a composite cylindrical shell. Table 2 lists results for buckling modes under pure shear (Cases 1–8) and combined shear and axial tension (Case 10) or compression (Case 9) of curved isotropic panels long in the circumferential direction (Cases 1–4), panels long in the axial dierection (Cases 6–8), and squarish panels (Cases 5, 9, 10). For panels long in the circumferential direction PANDA predictions agree very well with the predictions of Simitses *et al.*[52], which are based on multi-term, two-dimensional trigonometric expansions. PANDA overestimates the shear buckling loads for curved panels that are thin and long in the axial direction (Cases 6–8). (The result of Simitses *et al.*[52] for Case 8 is confirmed by a

Table 2. Buckling of monocoque cylindrical panels under pure shear

Case	$Z = \frac{a^2(1-\nu^2)^{1/2}}{Rt}$ (t = 1.0)	R	a/b	$[k_x^o]^*$	$k_s = N_{xy}^{cr}\, a^2 12(1-\nu^2)/(\pi^2 Et^3)$ PANDA (m,n,c or d)	Simitses [52]
1	10	100	0.187	0	8.15 (1,7,d=1.47)	7.90
2	100	100	0.187	0	29.41 (1,17,d=2.11)	29.01
3	1000	2000	0.187	0	159.8 (1,36,d=3.65)	162.00
4	2000	2000	0.187	0	268.9 (1,43,d=4.38)	266.00
5	100	100	1.000	0	29.22 (1,3,d=2.114)	34.73
6	100	100	5.000	0	163.93 (4,1,c=0.681)	148.30
7	100	100	10.00	0	577.8 (8,1,c=0.681)	564.90
8	1000	2000	10.00	0	950.9 (4,1,c=0.981)	700.00
9	1	100	0.667	-1.8	2.0045 (1,1,d=2.537)	2.956
10	1	100	0.667	+1.8	8.0853 (1,2,d=1.468)	9.572

* $k_x^o = N_{XPRE}\, a^2\, 12(1-\nu^2)/(\pi^2 Et^3)$

linear bifurcation analysis performed with use of STAGSC-1[53]). PANDA underestimates shear buckling loads for curved panels that are squarish and that buckle in less than three half waves in the "long" direction. (Cases 5, 9, 10.) This underestimation is due to violation of the simply supported boundary conditions along the two short edges.

Figure 9 shows buckling loads of an axially compressed, three-layered composite cylinder with an unbalanced laminate. Results from PANDA, STAGSC-1[53], and the analysis of Booton and Tennyson[54] are superposed. The STAGSC-1 results correspond to a two-dimensionally discretized finite element model and linear bifurcation with the assumption of a uniform membrane prebuckling state. Results from the rigorous STAGSC-1 analysis and the approximate PANDA analysis are in excellent agreement.

Stiffened axially compressed cylindrical shells. Table 3 lists bifurcation buckling load factors for an axially compressed, simply-supported, ring and stringer stiffened complete elastic cylindrical shell with various combinations of external and internal stiffening. The

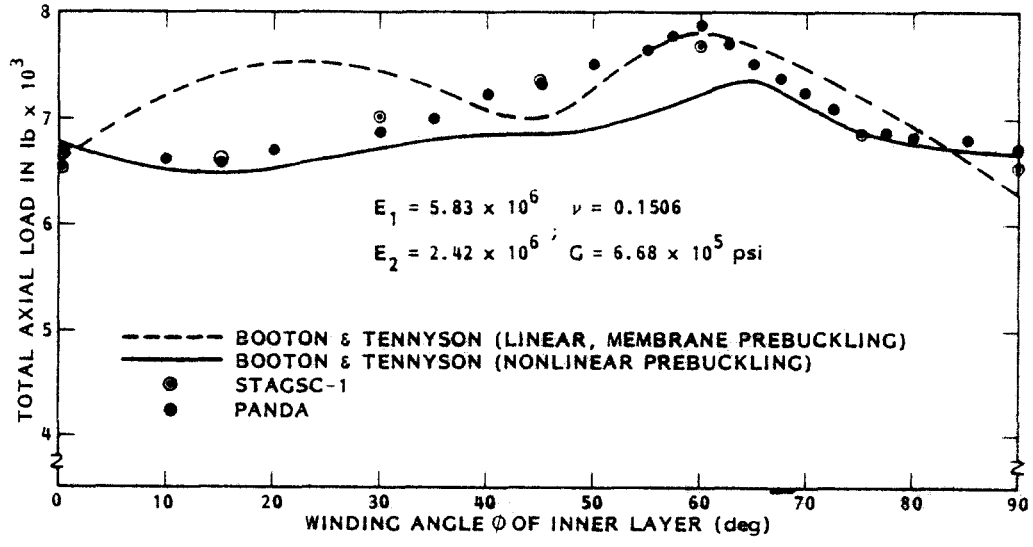

WINDING ANGLES OF INNER, MIDDLE, OUTER LAYERS = [Φ, 0, -Φ]
EACH LAYER = 0.0089 IN. THICK; CYLINDER RADIUS = 2.67 IN.;
LENGTH = 3.776 IN.

Fig. 9. Buckling loads of a composite, axially compressed cylindrical shell with an unbalanced laminate ($\phi, 0, -\phi$). Comparison of results from PANDA, STAGSC-1[53], and Booton and Tennyson[54].

Table 3. Comparison of PANDA buckling load predictions with those of other analyses for an axially-compressed cylinder with smeared rings and stringers (Fig. 10)

Case	Position of Stiffeners	NORMALIZED BUCKLING LOAD, $(N_x/E\bar{t})$ [a]		
		PANDA	NASA-TND-2960 [55]	Kicher & Wu [56]
1	Rings External Stringers External	0.004225(2,8) [b]	0.004137(3,8)	0.004270(-,7)
2	Rings Internal Stringers External	0.003544(3,8)	0.003574(3,8)	0.003562(-,8)
3	Rings External Stringers Internal	0.003025(3,8)	----------	0.003022(-,8)
4	Rings Internal Stringers Internal	0.002729(3,8)	0.002779(2,8)	0.002787(-,8)

[a] $\bar{t} = t_{shell} + (Area_{stringer}/b_{stringer}) = 0.244$ in.

[b] Numbers in parentheses are (axisl half-waves, circumferential full waves) over cylinder.

geometry and material properties are given in Fig. 10. Excellent agreement is obtained with the analyses of Block *et al.*[55] and Kicher and Wu[56].

Examples of buckling including stiffener rolling. Figure 11 and Table 4 pertain to an example which involves many of the types of instability listed in Table 1. The configuration is depicted in Fig. 11 and the buckling load factors predicted with PANDA are listed in Table 4. Comparisons between BOSOR4 and PANDA are plotted in Fig. 11, which is adapted from a figure in Ref. [57]. (The various curves labelled (1)–(6) in Fig. 11 are discussed in [57].)

The agreement with the 3-branch shell model of BOSOR4[58] is very good for all modes except the nonsymmetric ring sidesway mode with six circumferential waves, for which PANDA predicts a critical load about 14% higher than that predicted by BOSOR4.

In addition to the buckling load factors and critical wave numbers, which are provided as output from PANDA, the equation numbers from Ref. [51] on which the calculations are based are listed in Table 4.

The general instability eigenvalue, 949, corresponds to a buckling mode with one-half axial wave spanning the cylinder length of 200 in. The local skin buckling eigenvalue, 738, corresponds to buckling of a radially compressed, simply-supported, unstiffened, short cylinder (length = ring spacing = 25 in.) carrying a circumferential load N_y^0 (skin) = 90.7 lb/in., which is the share of the total circumferential resultant N_y^0 = 100 lb/in. that is carried by the skin midway between rings.

The load factors, 1113, 3645, 3645, corresponding to buckling of ring segments 1, 2, 3, respectively, are calculated from the assumptions that:

(1) The cross section of the T-shaped ring is considered to consist of three segments, of which the web is segment no. 1 and each half of the flange is a separate segment. (In PANDA stiffener cross sections are built up from assemblages of rectangular segments that must be joined end-to-end.)

(2) The web buckles as if it were a straight flat plate simply supported along its long edges (Fig. 3) and loaded in axial compression (normal to the plane of the page in Fig. 3) by 32.5 lb/in., which is its share of the total circumferential load as determined from the prebuckling analysis.

(3) The flange buckles with the same number of cir-

Table 4. Buckling load factors for externally pressurized, ring stiffened cylinder with radius = 100 in., thickness = 1.0 in., length = 200 in., $N_x^0 = 0$, $N_y^0 = 100$ lb/in. (Geometry shown in Fig. 11. Internal rings are spaced at 25 in. apart and both webs and flange are of thickness 0.4 in.)

Type of Buckling	Buckling Load Factor (Eigenvalue)	Circ. Full Waves	Governing Equations in Reference [51]	Is a Point Plotted in Fig. 11?
General instability	949	3	57 (smeared rings)	Yes
Local skin buckling	738	16	57 (no rings)	Yes
Buckling of ring seg. 1	1113	39	71 (web buckling)	No
Buckling of ring seg. 2	3645	39	79 (flange buckling)	No
Buckling of ring seg. 3	3645	39	79 (flange buckling)	No
Local rolling with skin buckling between rings	707	15	57 (with 96 and 97)	Yes
Rolling of rings, no skin buckling	811	6	112 (web), 119 (flange)	Yes
Axisymmetric rolling of rings, no skin buckling	1320	0	112 (web), 119 (flange)	Yes

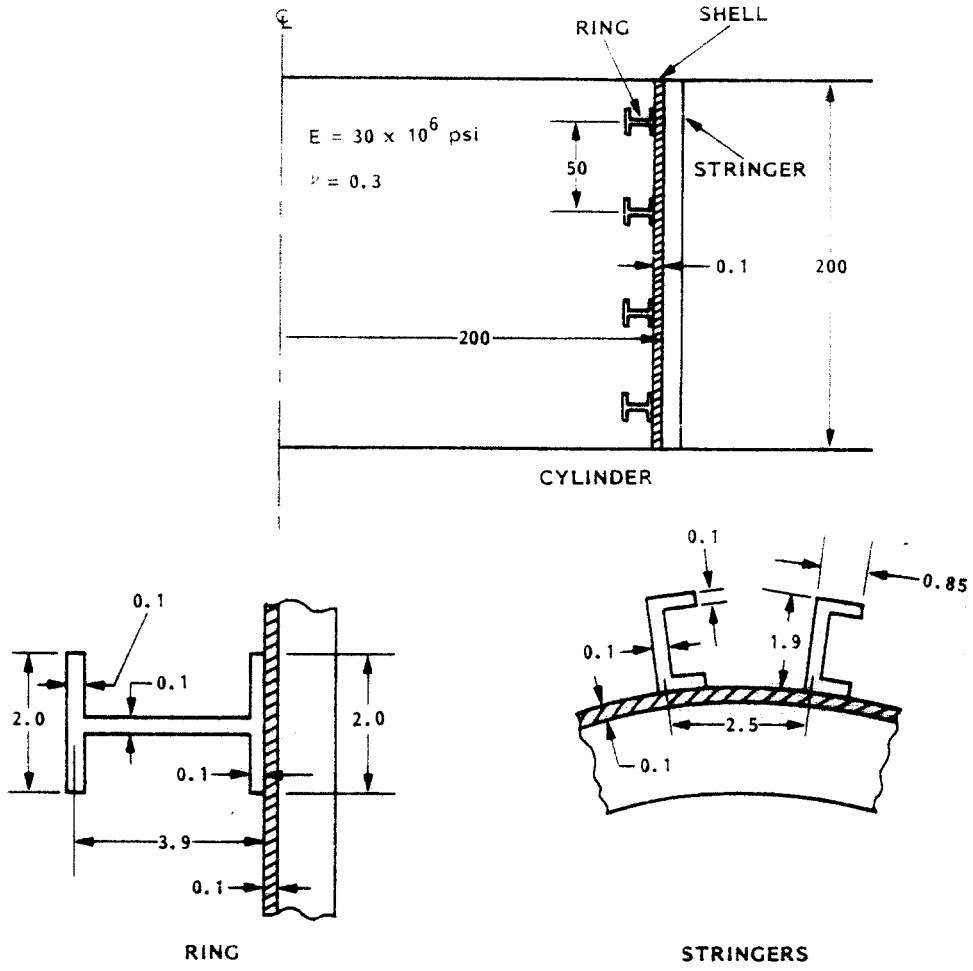

Fig. 10. Axially compressed ring and stringer stiffened cylindrical shell analysed by Block *et al.*[55] and by Kicher and Wu[56]. (See Table 3.)

cumferential waves, 39, as that for local buckling of the web.

The load factor, 707, corresponding to local rolling with skin buckling between stiffeners (see Fig. 4a) is actually the best estimate of local buckling in this case because the local skin buckling load factor, 738, is calculated neglecting two counteracting effects contributed by the rings:

(1) the resistance of the rings to twisting about their attachment line to the skin (strain energy of ring rolling), which of course would tend to increase the load factor, and

(2) the work done by the prebuckling compression along the ring axes as the rings deform in the buckling mode, which would tend to decrease the load factor.

In this case the approximate local skin buckling load factor of 738, based on the assumption of simple support along ring lines of attachment, is slightly unconservative because the "work done" contribution (2) outweighs the ring rolling strain energy (1). The significant effect of these terms has been discussed previously. (See Ref. [57], in particular Figs. 4 and 7 and the associated discussion in [57].)

The load factor, 811, in Table 4 corresponds to buckling deformations of the type shown in Fig. 4(b), in which the cross section of the web deforms but the skin does not participate. As seen from Fig. 11, PANDA overestimates the load factor corresponding to this mode by about 14%. The load factor, 1320, corresponding to axisymmetric rolling (Fig. 4c) is also somewhat higher than the prediction from BOSOR4 for the same mode (zero circumferential waves).

Were the ring stiffened cylinder to be optimized, all of the buckling load factors appearing in Table 4 might constrain the design at various iterations during the optimization process. The question arises, why include both the local skin buckling (738) and local rolling with skin buckling between rings (707) as potential constraints on the optimization process when the latter load factor seems to represent a more rigorous model of the actual phenomenon than the former? The answer is that the accuracy with which the various load factors are determined is case dependent. All of the formulas given in Ref. [51] are approximate. For different dimensions or for cases involving nonlinear material behavior the local-rolling-with-skin-buckling model may not yield as accurate a result as that from the local skin buckling model.

This statement holds especially for cases involving stiffeners with slender webs and stocky flanges, cases in which there is more than one half wave between stiffeners in the critical buckling modes, and cases in which local plastic flow along the stiffener attachment

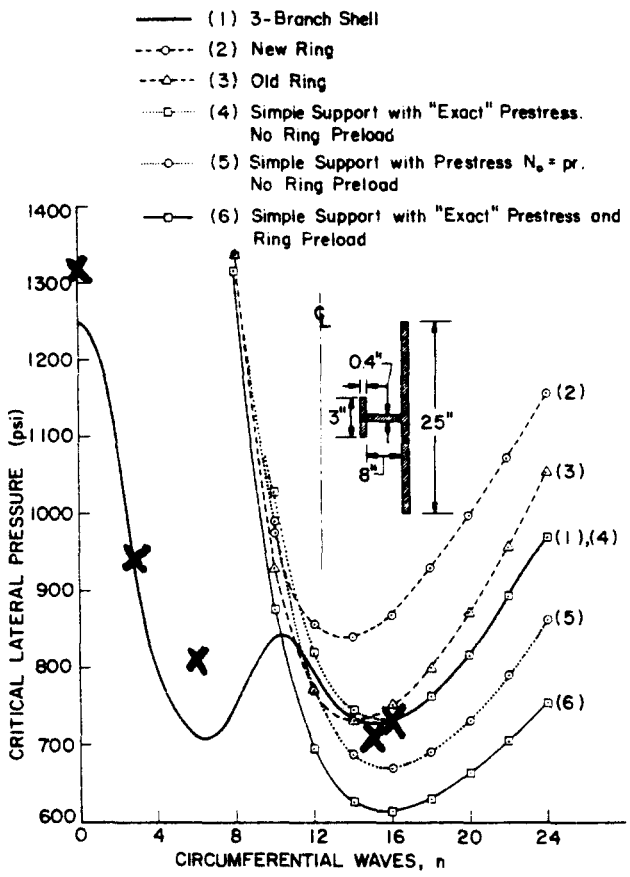

Fig. 11. Local and general buckling of ring stiffened cylinder under uniform lateral external pressure. Solid line is from BOSOR4 predictions; x's are from PANDA. (See Table 4.)

line occurs before buckling. If the web is slender or if there is more than one half wave between stiffeners in any of the buckling modes, the stiffener-rolling-with-skin-buckling model will overestimate the influence of the stiffener rolling terms. In cases involving prebuckling plastic flow, plastic hinges may form at stiffener lines of attachment, perhaps rendering the local-skin-buckling model with simple supports at stiffener lines of attachment, a better representation of the actual local buckling phenomenon than the more complex local-rolling-with-skin-buckling model, even for modes with only one half wave between stiffeners in either or both of the coordinate directions. Since computer time is not especially important in applications of PANDA, it is safest to include estimates for all of the possible buckling modes as constraints in the optimization process.

Other examples. Many other examples of buckling of fixed designs are given in Ref. [51]. These are compared with results in the literature.

Optimum designs obtained with PANDA

Tables 5 and 6 give results of the application of PANDA to problems that have previously been solved by Simitses *et al.*[33, 52]. The two examples involve stiffened complete (360 deg.) cylindrical shells. These are modelled in applications of PANDA as deep cylindrical "panels" that span 180 deg. Such a model, given the simple support condition along diametrically opposed generators, is equivalent to treatment of the full 360 deg. cylindrical shell: the number of half waves along the circumferential coordinate of the 180 deg. "panel" is equivalent to the number of full waves around the circumference of the complete cylinder.

Each of Tables 5 and 6 is horizontally divided into three sections: dimensions, design load combination and material properties are given in the top section; weight and decision variables for optimization are listed in the middle section and buckling load factors and wave numbers are listed in the bottom section. Optimum designs from PANDA are listed on the left and those from the referenced analysis are listed on the right. Buckling load factors and modes for both left and right sides were calculated with PANDA.

The data in each of Tables 5 and 6 were generated in the following way: Simple buckling analyses were first performed with PANDA, corresponding to the dimensions found by the referenced investigation to be an optimum design. The dimensions found to be optimum by the referenced investigation and the buckling load factors and modes computed by PANDA corresponding to these dimensions are listed in the right-hand columns of Tables 5 and 6. These "optimum" designs were then used as starting designs in the optimization process with PANDA. Through execution of the program module "DECIDE", the design variables listed in Tables 5 and 6 were chosen as decision variables for the optimization analysis with PANDA. Following execution of "DECIDE", the program module "PANCON" was run again, this time in the optimization mode. The results listed in the left-hand columns represent the converged

Table 5. Comparison of optimum designs obtained from PANDA and from the analysis of Ref. [33] for an axially compressed ring and stringer stiffened cylindrical shell.

CYLINDER RADIUS, R = 95.5 in.; CYLINDER LENGTH, L = 291 in.;
AXIAL RESULTANT, N_x^o = -800 lb/in.;
YOUNG'S MODULUS, E = 10.5 x 10^6 psi; POISSON'S RATIO, NU = 0.33; DENSITY = 0.101 lb/in^3;
MINIMUM GAGE OF ANY THICKNESS = 0.02 in.
BOTH STRINGERS AND RINGS INTERNAL AND OF RECTANGULAR CROSS SECTION

OPTIMUM DESIGN AND BUCKLING LOAD FACTORS AND MODES:	FROM PANDA	FROM REF. [33]
PANEL WEIGHT (180° OF CYLINDER) =	3.4893E+02	3.7796E+02
DESIGN VARIABLES FOR ITERATION NUMBER 0 FOLLOW...		
THICKNESS OF PANEL SKIN LAYER NO. 1 =	2.1701E-02	2.2105E-02
STRINGER SPACING, B =	8.9191E-01	9.1985E-01
THICKNESS OF STRINGER SEGMENT NO. 1 =	2.6267E-02	3.2620E-02
WIDTH, BS(I), OF STRINGER SEGMENT 1 =	4.5089E-01	4.4210E-01
RING SPACING, A =	9.4767E+00	9.3871E+00
THICKNESS OF RING SEGMENT NO. 1 =	2.0000E-02	2.2720E-02
WIDTH, BR(I), OF RING SEGMENT 1 =	2.1766E+00	2.1000E+00
(M=AXIAL, N=CIRC.) HALF-WAVES OVER ENTIRE PANEL (AXIAL,CIRC.)		(AXIAL,CIRC.)
GENERAL INSTABILITY EIGENVALUE(M,N)=	9.9691E-01(18, 9)	1.0432E+00(17, 9)[a]
LOCAL SKIN (BUCKLING/PHI) (M,N) =	9.9299E-01(337, 336)	1.0425E+00(309, 326)[a]
BUCKLING BETWEEN RINGS WITH SMEARD STRINGRS=	1.0012E+00(30, 36)	1.1181E+00(30, 36)[a]
BUCKLING BETWEEN STRINGRS WITH SMEARD RINGS=	4.3916E+01(3057, 336)	4.5582E+01(2946, 326)
BUCKLING/PHI (M) OF STRINGER SEGMENT NO. 1=	1.0004E+00(337)	1.6029E+00(309)
LOCAL ROLLING WITH SKIN BUCKLING BETWN STIF=	6.2211E+00(276, 336)	6.2724E+00(247, 326)
ROLLING OF STRINGERS(M,0), NO SKIN BUCKLING=	1.9307E+00(404, 0)	3.3449E+00(404, 0)
AXISYMMETRIC ROLLING OF RINGS, NO SKIN BUCK=	1.0000E+23(0, 0)	1.0000E+23(0, 0)
BUCKLING(ROLLING) MODE WITH SMEARD STRINGRS=	1.0098E+00(30, 36)	1.1271E+00(30, 34)
BUCKLING(ROLLING) MODE WITH SMEARED RINGS =	3.9001E+01(2752, 336)	4.4407E+01(2358, 326)

[a]These loads and modes are predicted by PANDA for the optimum design obtained by the computer analysis described in [33]. The load factors and modes predicted by the Ref. [33] are, respectively, 1.000(18,9), 1.048(-,-), and 1.109(30,36).

Table 6. Comparison of optimum designs obtained from PANDA and from the analysis of Ref. [52] for a ring and stringer-stiffened cylindrical shell under combined axial compression and torsion

CYLINDER RADIUS, R = 65.0 in.; CYLINDER LENGTH, L = 100 in.;
AXIAL, SHEAR STRESS RESULTANTS, N_x^o = -2700 lb/in.; N_{xy}^o = 418.5 lb/in.;
YOUNG'S MODULUS, E = 10.5 x 10^6 psi; POISSON'S RATIO, NU = 0.33; DENSITY = 0.101 lb/in^3;
MAXIMUM STRESS = 45 ksi; MINIMUM GAGE OF ANY THICKNESS = 0.05 in.;
INTERNAL STRINGERS WITH T-SHAPED CROSS SECTION; INTERNAL RINGS WITH RECTANGULAR CROSS SECTION.

OPTIMUM DESIGN AND BUCKLING LOAD FACTORS AND MODES:	FROM PANDA	FROM REF. [52]
PANEL WEIGHT (180° OF CYLINDER) =	2.2961E+02	2.4301E+02
DESIGN VARIABLES FOR ITERATION NUMBER 0 FOLLOW...		
THICKNESS OF PANEL SKIN LAYER NO. 1 =	5.0000E-02	5.0000E-02
STRINGER SPACING, B =	1.6054E+00	1.6086E+00
THICKNESS OF STRINGER SEGMENT NO. 1 =	5.0000E-02	5.0120E-02
THICKNESS OF STRINGER SEGMENT NO. 2 =	7.3997E-02	5.0120E-02
WIDTH, BS(I), OF STRINGER SEGMENT 1 =	7.1470E-01	6.5738E-01
WIDTH, BS(I), OF STRINGER SEGMENT 2 =	1.9535E-02	9.8605E-02
RING SPACING, A =	1.2284E+01	9.0909E+00
THICKNESS OF RING SEGMENT NO. 1 =	5.0000E-02	5.1630E-02
WIDTH, BR(I), OF RING SEGMENT 1 =	2.7232E+00	2.3750E+00
(M=AXIAL, N=CIRC.) HALF-WAVES OVER ENTIRE PANEL (AXIAL,CIRC.)		(AXIAL,CIRC.)
GENERAL INSTABILITY EIGENVALUE(M,N)=	9.9963E-01(1, 8)	1.0121E+00(1, 8)[a]
LOCAL SKIN (BUCKLING/PHI) (M,N) =	9.9984E-01(65, 166)	1.0285E+00(65, 165)[a]
BUCKLING BETWEEN RINGS WITH SMEARD STRINGRS=	1.0062E+00(8, 26)	2.0912E+00(10, 28)[a]
BUCKLING BETWEEN STRINGRS WITH SMEARD RINGS=	2.5461E+01(436, 166)	2.5254E+01(428, 165)
BUCKLING/PHI (M) OF STRINGER SEGMENT NO. 1=	5.3301E+00(138)	6.5595E+00(142)
BUCKLING/PHI (M) OF STRINGER SEGMENT NO. 2=	1.5940E+03(138)	3.1326E+01(142)
BUCKLING/PHI (M) OF STRINGER SEGMENT NO. 3=	1.5940E+03(138)	3.1326E+01(142)
LOCAL ROLLING WITH SKIN BUCKLING BETWN STIF=	1.1231E+00(56, 166)	1.5011E+00(43, 165)
ROLLING OF STRINGERS(M,0), NO SKIN BUCKLING=	1.5450E+00(84, 0)	3.0057E+00(45, 0)
AXISYMMETRIC ROLLING OF RINGS, NO SKIN BUCK=	1.0000E+23(0, 0)	1.0000E+23(0, 0)
BUCKLING(ROLLING) MODE WITH SMEARD STRINGRS=	1.0170E+00(8, 26)	2.1131E+00(10, 28)
BUCKLING(ROLLING) MODE WITH SMEARED RINGS =	1.3474E+01(393, 166)	2.5362E+01(278, 165)
MARGIN FOR EFFECTIVE STRESS IN LAYER 1 =	1.1795E+00	1.2174E+00
MARGIN FOR COMP. STRAIN IN STRINGER SEG. 1=	1.2642E+00	1.3100E+00
MARGIN FOR COMP. STRAIN IN STRINGER SEG. 2=	1.2642E+00	1.3100E+00
MARGIN FOR COMP. STRAIN IN STRINGER SEG. 3=	1.2642E+00	1.3100E+00

[a]The analysis of Ref. [52] yields, respectively, for these modes: 1.0(1,8), 1.048(-,-), & 20.8(10,30

optimum designs from PANDA. They are generally obtained after two or three sets of five iterations each, requiring a total of about a minute on the VAX 11/780 computer.

Table 5. The minimum weight and buckling loads from PANDA agree rather well with those from the analysis of Ref. [33]. In the PANDA design the stringer is quite a bit thinner than is the case in the Ref. [33] optimum. This difference arises from the way that local stringer (or ring) buckling is handled (see the fifth load factor from the top, 1.6029 for the Ref. [33] dimensions): In both codes the stiffeners are assumed to be simply supported along their lines of attachment to the shell. However, in PANDA, for stiffeners of rectangular cross section, the number of waves along the stiffener axis must be equal to that governing local buckling of the skin. Inclusion in PANDA of the modes with the word "rolling" in them compensates for any unconservativeness that may be present because of this approach. In many other codes, including that on which the results of Ref. [33] are based, the minimum buckling load with respect to the number of waves along the stiffener axis is found without regard to the compatibility of stiffener and shell rotations. This minimum usually occurs at a lower wave number than that corresponding to local skin buckling, and at a lower stress, leading to the appearance of a need for stockier stiffeners.

Table 6. This case involves combined axial compression and torsion, and it is primarily the axial compression load component that "designs" the structure. The results from PANDA and Ref. [52] show reasonably good agreement. Note that certain stress and strain constraints are printed out at the bottom of the table. These are printed by PANDA whenever they are less than 2.0.

Other examples. Many other examples of optimized panels and shells are presented in Ref. [51]. These are compared with results in the literature.

CONCLUSIONS

Accuracy with which buckling loads are computed by PANDA

The PANDA system was developed on a minicomputer. In order to obtain interactively optimum designs of stiffened panels in the presence of many decision variables and many buckling constraints, buckling loads and mode shapes have to be calculated extremely rapidly. Therefore, buckling formulas are derived from simple assumed displacement fields, such as those for the shell in eqns (1) or (2) and for the stiffeners in eqns (3) and (4).

Cases in which the assumed displacement patterns lead to rather poor estimates of the buckling loads are described in Ref. [51]. They include buckling of certain unstiffened curved panels under pure in-plane shear (Table 2, Cases 8–10); buckling under pure axial compression of a wide, short, stiffened panel (Fig. 22(c) of Ref. [51]); and rolling instability of the internal rings of a radially compressed cylindrical shell (Fig. 11). It is felt, however, that so many buckling constraints are included in the optimization analysis that at or near the optimum design the degree of unconservatism inherent in the one-term Ritz-type analysis on which PANDA is based has less impact than might appear to be the case from a simple buckling analysis of a non-optimized design.

In order to compensate for possible unconservativeness in the PANDA analysis, the user should:

(1) increase the in-plane loads to which the panel is being designed and,

(2) check the load-carrying capability of the optimum design obtained with PANDA with use of a more rigorous buckling analysis, such as provided by a finite element program (Refs. [48, 53, 58, 59]).

Even if the approximate nature of the buckling analysis in PANDA is disregarded, the loads applied in the design analysis must be greater than the operating loads in order to compensate for initial imperfections, which are not other wise accounted for. The failure of PANDA to predict accurate buckling loads in all situations is less significant when viewed from this perspective. It should also be emphasized that PANDA is intended to be used for *preliminary* design.

In a few instances discrepancies between the buckling predictions of PANDA and those from the literature were investigated further with the use of BOSOR4[58], BOSOR5[59] or STAGSC-1[53]. The predictions from these more rigorous computer codes often tend to confirm the PANDA results[51]. Particularly good agreement is exhibited between PANDA and BOSOR5 for elastic–plastic buckling of optimized, hydrostatically compressed, ring-stiffened cylindrical shells optimized for external pressures from about 700 to about 4700 psi. See Ref. [51] for details.

How PANDA performs on the VAX computer

PANDA operates at a reasonable speed for interactive computing on a minicomputer such as the VAX 11/780. For example, the optimum design of the ring and stringer-stiffened cylindrical shell to which the results in Table 6 correspond, is obtained in four sets of five iterations each. Each set requires about 20 sec at the terminal. This means that every 4 sec a new design is generated as iterations progress toward the optimum, a reasonable speed at which to obtain optimum designs in a conversationally interactive mode.

Possible future enhancements of the capability of PANDA

There are many ways in which PANDA could be improved with retention of its computationally interactive nature:

(1) The effect of imperfections could be incorporated explicitly in PANDA through the use of semiempirical formulas of the type derived by Miller and Tsai for the ASME code[60], for example.

(2) New buckling modal displacement functions could be introduced such that other than simple support boundary conditions could be imposed. This would be especially important for the case of axially stiffened panels clamped at the edges and buckling in the general instability mode. In order to obtain reasonably optimum designs for a test environment, in which the loaded edges are usually clamped rather than simply supported, one would have to be able to apply clamping for the general instability mode and simple support for the local modes.

(3) Optimization could be performed for ranges of in-plane load components, rather than just for a single in-plane load combination. This might be done by first computing the buckling load interaction surfaces

$$f(N_x^0, N_y^0, N_{xy}^0) = 0 \tag{5}$$

for each type of buckling mode that span the range of load components provided by the program user and then

introducing only that load combination for each buckling mode which is most critical relative to the corresponding load interaction surface.

(4) PANDA could be expanded to handle other than cylindrical geometry. Here the difficult task would be to choose appropriate displacement functions for the approximate buckling analysis.

(5) The general instability analysis could be improved in the case of stiffened panels by use of a more elaborate assumed displacement field, one that reflects the local-general nature of general instability buckling modes such as that shown in Fig. 22(c) of Ref. [51]. Such an improvement would require of PANDA the capability to handle the stiffeners as discrete in calculations of general or semi-general instability load factors and mode shapes.

(6) Panels for aircraft fuselages and ship decking are often designed so that local buckling of the skin between adjacent stiffeners is permitted. PANDA could be improved by use of effective stiffness of the skin in its post-buckled state. A difficult task here would be to calculate maximum strains in the loaded, post-buckled skin.

(7) Composite materials exhibit a great variety of failure modes and some nonlinear material behavior. Some of this new knowledge should be incorporated into PANDA, which, in the case of anisotropic laminates, now simply checks for maximum stress or strain of each layer and is restricted to linear material behavior if the material is orthotropic.

(8) Sanders' equations could be used rather than Donnell's.

(9) The scope of PANDA could be broadened to include optimization with respect to individual lamina properties of laminated stiffeners.

(10) PANDA is now limited to the analysis of panels with open-section stiffeners. The capability could be expanded to permit optimization of corrugated panels or panels with hat stiffeners.

Acknowledgements—Part of the effort to develop PANDA was sponsored by the U.S. Air Force, Aeronautical Systems Division, Wright Patterson AFB, Ohio, under Contract AFFDL F33615-76-C-3105. Dr. Narenda S. Khot (AFWAL/FIBRA) was project engineer. Much of the support for the development of PANDA came from the 1980–1982 Lockheed Independent Development Programs. For this support the auther is greatly indebted to Bill Sable. Some of the support for production of this paper was provided by the 1982 Lockheed Independent Research Program.

REFERENCES

1. L. H. Donnell, A new theory for the buckling of a thin cylinder under axial compression and bending. *Trans. ASME* **56**(11), 795–806 (1934).
2. G. N. Vanderplaats, "CONMIN—a FORTRAN program for constrained function minimization. NASA TM X-62-282, version updated in March 1975, Ames Research Center, Moffett Field, California (Aug. 1973).
3. G. N. Vanderplaats and F. Moses, Structural optimization by methods of feasible directions. *Comput. Structures* **3**, 739–755 (1973).
4. G. Zoutendijk, *Methods of Feasible Directions*. Elsevier, Amsterdam (1960).
5. V. B. Venkayya, Structural optimization: a review and some recommendations. *Int. J. Num. Meth. Engng* **13**, 203–228 (1978).
5a. E. J. Catchpole, The optimum design of compression surfaces having unflanged integral stiffeners. *J. Roy. Aerospace Society* **58**, 765 (1954).
6. L. A. Schmit, T. P. Kicher and W. M. Morrow, Structural synthesis capability for integrally stiffened waffle plates. *AIAA J.* **1**, 2820–2836 (1963).
7. W. M. Morrow and L. A. Schmit, Structural synthesis of a stiffened cylinder. *NASA CR*-1217 (Dec. 1968).
8. T. P. Kicher, Structural synthesis of integrally stiffened cylinders. *J. Spacecraft and Rockets* **5**, 62–67 (1968).
9. L. D. Hofmeister and L. P. Felton, Synthesis of waffle plates with multiple rib sizes. *AIAA J.* **5**, 2193–2199 (1969).
10. R. J. Bronowicki, R. B. Nelson, L. P. Felton and L. A. Schmit, Jr., Optimization of ring stiffened cylindrical shells. *AAIA J.* **13**, 1319–1325 (1975).
11. R. F. Crawford and A. B. Burns, Minimum weight potentials for stiffened plates and shells. *AIAA J.* **1**, 879–886 (1963).
12. A. B. Burns and J. Skogh, Combined loads minimum weight analysis of stiffened plates and shells. *J. Spacecraft and Rockets* **3**, 235–240 (1966).
13. A. B. Burns and B. O. Almroth, Structural optimization of axially compressed cylinders, considering ring-stringer eccentricity effects. *J. Spacecraft and Rockets* **3**, 1263–1268 (1966).
14. A. B. Burns, Optimum stiffened cylinders for combined axial compression and internal or external pressure. *J. Spacecraft and Rockets* **5**, 690–699 (1968).
15. B. O. Almroth, A. B. Burns and E. V. Pittner, Design criteria for axially loaded cylindrical shells. *J. Spacecraft and Rockets* **7**, 714–720 (1970).
16. G. A. Cohen, Optimum design of truss-core sandwich cylinders under axial compression. *AAIA J.* **1**, 1626–1630 (1963).
17. G. Gerard, Optimum structural design concepts for aerospace vehicles. *J. Spacecraft and Rockets* **3**, 5–18 (1966).
18. W. J. Stroud and N. P. Sykes, Minimum-weight stiffened shells with slight meridional curvature designed to support axial compressive loads. *AIAA J.* **7**, 1599–1601 (1969).
19. C. Lakshmikantham and G. Gerard, Minimum weight design of stiffened cylinders. *Aerospace Quarterly* 49–68 (Feb. 1970).
20. D. L. Block, Minimum weight design of axially compressed ring and stringer stiffened cylindrical shells. *NASA CR*-1766 (July 1971).
21. J. L. Shideler, M. S. Anderson and L. R. Jackson, Optimum mass-strength analysis for orthotropic ring-stiffened cylinders under axial compression. *NASA TND*-6772 (July 1972).
22. A. V. Viswanathan and M. Tamekuni, Elastic buckling analysis for composite stiffened panels and other structures subjected to biaxial inplane loads. *NASA CR*-2216 (Mar. 1973).
23. W. H. Wittrick and F. W. Williams, Buckling and vibration of anisotropic or isotropic plate assemblies under combined loadings. *Int. J. Mech. Sci.* **16**, 209–239 (1974).
24. J. G. Williams and M. Stein, Buckling behavior and structural efficiency of open-section stiffened composite compression panels. *AIAA J.* **14**, 1618–1626 (1976).
25. B. L. Agarwal and L. H. Sobel, Weight comparisons of optimized stiffened, unstiffened and sandwich cylindrical shells. *J. Aircraft* **14**, 1000–1008 (1977).
26. M. S. Anderson and W. J. Stroud, General panel sizing computer code and its application to composite structural panels. *AIAA J.* **17**, 892–897 (1979).
27. G. G. Weaver and J. R. Vinson, Minimum-mass designs of stiffened graphite/polymide compression panels. In *Modern Developments in Composite Materials and Structures*. pp. 215–233, ASME 1979 Winter Annual Meeting (Dec. 1979).
28. L. A. McCullers, Automated design of advanced composite structures. *ASME AMD*, **7**, 119–130 (Nov. 1974).
29. T. Hayashi, Optimization for elastic buckling strength of fiber-reinforced composite structures-columns, plates and cylinders. *Proc. Mech. Behavior of Materials*. pp. 399–405. Society of Material Science, Japan (Aug. 1974).
29a. M. Aswani, Optimization of stiffened cylinder subject to destabilizing load. *Proc. Advances in Civil Engng Through Engng. Mech.*, pp. 456–459. ASCE, New York (May 1977).
30. N. S. Khot, Computer Program (OPTCOMP) for optimization of composite structures for minimum weight design. *AFFDL-TR*-76-149 (1977).

31. J. H. Starnes, Jr. and R. T. Haftka, Preliminary design of composite wings for buckling strength, and displacement constraints. *J. Aircraft*, **16**, 564–570 (1979).
32. G. J. Simitses and V. Ungbhakorn, Weight optimization of stiffened cylinders under axial compression. *Comput Structures* **5**, 305–314 (1975).
33. G. J. Simitses and V. Ungbhakorn, Minimum-weight design of stiffened cylinders under axial compression. *AIAA J.* **13**, 750–755 (1975).
34. I. Sheinman and G. J. Simitses, Buckling analysis of geometrically imperfect stiffened cylinders under axial compression. *AIAA J.* **15**, 374–382 (1977).
35. G. J. Simitses and J. Giri, Optimum weight design of stiffened cylinders subjected to torsion combined with axial compression with and without lateral pressure. *Comput. Structures* **8**, 19–30 (1978).
36. G. J. Simitses and I. Sheinman, Optimization of geometrically imperfect stiffened cylindrical shells under axial compression. *Comput Structures* **9**, 377–381 (1978).
37. J. N. Dickson, S. B. Biggers and J. T. S. Wang, A preliminary design procedure for composite panels with open-section stiffeners loaded in the post-buckling range. In *Advances in Composite Material*, Vol. 1, pp. 812–825. Pergamon Press, Oxford (1980).
38. W. T. Koiter, Het schuifplooiveld by grote over-schrydingen van de knikspanning. *NLL Report* S295 (Nov. 1946).
39. J. B. Caldwell and A. D. Hewitt, Cost effective design of ship structures. *Met. Constr.* **8**, 64–67 (1976).
40. J. G. Pulos and M. A. Krenzke, Recent developments in pressure hull structures and materials for hydrospace vehicles. *David Taylor Model Basin Rep.* 2137, Washington, D.C. (Dec. 1965).
41. M. E. Lunchick, Plastic axisymmetric buckling of ring-stiffened cylindrical shells fabricated from strain-hardening materials and subjected to external hydrostatic pressure. *David Taylor Model Basin Rep.* 1393, Washington, D.C. (Jan. 1961).
42. M. E. Lunchick, Plastic general-instability pressure of submarine pressure hulls. *ASME Paper* 62-*WA*-262 (1962).
43. L. Boichot and T. E. Reynolds, Inelastic buckling tests of ring-stiffened cylinders under hydrostatic pressure. *David Taylor Model Basin Rep.* 1992, Washington, D.C. (May 1965).
44. J. R. Renzi, Optimization of orthotropic, non-linear, ring-stiffened cylindrical shells under external hydrostatic pressure as applied to mmc materials, Naval Surface Weapons Center, *NSWC TR* 79-305 (Sept. 1979). See also, J. R. Renzi, Axisymmetric stresses and deflections, inter-bay buckling, and general instability of orthotropic, hybrid, ring-stiffened cylindrical shells under external hydrostatic pressure, Naval Surface Weapons Center, *NSWC TR*-80-269 (April 1981).
45. M. Pappas and C. L. Amba-Rao, A direct search algorithm for automated optimum structural design. *AIAA J.* **9**, 387–393 (1971).
46. M. Pappas and A. Allentuch, Structural synthesis of frame reinforced submersible circular cylindrical hulls. *Comput. Structures* **4**, 253–280 (1974).
47. M. Pappas and A. Allentuch, Pressure hull optimization using general instability equation admitting more than one longitudinal buckling half-wave. *J. Ship Research* **19**, 18–22 (1975).
48. B. O. Almroth, P. Stern and D. Bushnell, Imperfection sensitivity of optimized structural panels. *AFWAL-TR*-80-3182 (Mar. 1981).
49. S. N. Patnaik and M. Maiti, Optimum design of stiffened structures with constraint on the frequency in the presence of initial stresses. *Comput. Meth. Appl. Mech. Engng* **7**, 303–322 (1976).
50. M. W. Dobbs and R. B. Nelson, Minimum weight design of stiffened panels with fracture constraints. *Comput. Structures* **8**, 753–759 (1978).
51. D. Bushnell, Panel optimization with integrated software (POIS), Volume 1: PANDA—Interactive program for preliminary minimum weight design, *Report No. AFWAL-TR*-81-3073, Flight Dynamics Laboratory, Air Force Wright Aeronautical Laboratories, Wright Patterson AFB, Ohio (July 1981).
52. G. J. Simitses, J. Giri and I. Sheinman, Minimum weight design of stiffened cylinders and cylindrical panels under combined loads. *AFOSR TR*-76-0930, Georgia Institute of Technology, Atlanta, Georgia (1976).
53. B. O. Almroth and F. A. Brogan, The STAGS computer code. NASA Langley Research Center, *NASA CR* 2950 (Feb. 1978).
54. M. Booton and R. C. Tennyson, Buckling of imperfect anisotropic circular cylinders under combined loading. *AIAA J.* **17**(3), 278–287 (Mar. 1979).
55. D. W. Block, M. F. Card and M. F. Mikulas, Jr., Buckling of eccentrically stiffened orthotropic cylinders. NASA Langley Research Center, *NASA TND* 2960 (Aug. 1965).
56. T. P. Kicher and C-H Wu, Buckling of anisotropic circular cylindrical shells. *AFML Rept. TR*-71-260 (Nov. 1971).
57. D. Bushnell, Evaluation of various analytical models for buckling and vibration of stiffened shells. *AIAA J.* **11**(9), 1283–1291 (1973).
58. D. Bushnell, Stress, stability and vibration of complex, branched shells of revolution. *Comput. Structures* **4**, 399–435 (1974).
59. D. Bushnell, BOSOR5—program for buckling of elastic-plastic complex shells of revolution including large deflections and creep. *Comput. Structures* **6**, 221–239 (1976).
60. C. D. Miller, Code Case N-284, *ASME Boiler and Pressure Vessel Code*, 1980 *Code Cases Nuclear Components*, pp. 633–656. American Society of Mechanical Engineers, New York (July 1980).